

Supporting Information

Predicted Stable Structures of the Li-Ag System at High Pressures

Xin Zhong*, Xue Li*, Lihua Yang, Dandan Wang, Xin Qu, Hanyu Liu*

Corresponding Authors

*E-mail: zhongxin@calypso.cn

*E-mail: lx@calypso.cn

*E-mail: hanyuliu@jlu.edu.cn

Xin Zhong - Key Laboratory of Functional Materials Physics and Chemistry of the Ministry of Education, Jilin Normal University, Changchun 130103, P. R. China; College of Physics, Jilin Normal University, Siping 136000, China; National Demonstration Center for Experimental Physics Education, Jilin Normal University, Siping 136000, China; orcid.org/0000-0003-3327-1045;
Email: zhongxin@calypso.cn

Xue Li - State Key Laboratory of Superhard Materials, College of Physics, Jilin University, Changchun 130012, China;
Email: lx@calypso.cn

Lihua Yang - Key Laboratory of Functional Materials Physics and Chemistry of the Ministry of Education, Jilin Normal University, Changchun 130103, P. R. China; College of Physics, Jilin Normal University, Siping 136000, China; National Demonstration Center for Experimental Physics Education, Jilin Normal University, Siping 136000, China

Dandan Wang - Key Laboratory of Functional Materials Physics and Chemistry of the Ministry of Education, Jilin Normal University, Changchun 130103, P. R. China; College of Physics, Jilin Normal University, Siping 136000, China; National Demonstration Center for Experimental Physics Education, Jilin Normal University, Siping 136000, China

Xin Qu - Key Laboratory of Functional Materials Physics and Chemistry of the Ministry of Education, Jilin Normal University, Changchun 130103, P. R. China; College of Physics, Jilin Normal University, Siping 136000, China; National Demonstration Center for Experimental Physics Education, Jilin Normal University, Siping 136000, China

Hanyu Liu - State Key Laboratory of Superhard Materials, International Center for Computational Method & Software, Key Laboratory of Physics and Technology for Advanced Batteries (Ministry of Education), College of Physics and International Center of Future Science, Jilin University, Changchun 130012, China; orcid.org/0000-0003-2394-5421;
Email: hanyuliu@jlu.edu.cn; lhy@calypso.cn

Index

1. Supplementary Computational Details.....	1
2. Comparison of PAW pseudopotentials and the LAPW method.....	2
3. Structure of stable Li-rich Li_mAg ($m=1-6$) at high pressure.....	3
4. Phonon spectra and dynamic stability.....	3
5. Two-dimensional ELF plots on (0 0 1) section of Li_4Ag	4
6. Comparison of PDOS of $5p$ orbital of Ag for Li_4Ag , Li_0In , and Li_0Sn	5
7. Detailed Structural Information	6

1. Supplementary Computational Details

Our structural prediction approach is based on a global minimization of free energy surfaces of given compounds by combining ab initio total-energy calculations with the particle swarm optimization (PSO) algorithm. The structure search of each Li_mAg_n ($m=1-6$, $n=1-6$) stoichiometry is performed with simulation cells containing 1–4 formula units. In the first generation, a population of structures belonging to certain space group symmetries are randomly constructed. Local optimizations of candidate structures are done by using the conjugate gradients method through the VASP code, with an economy set of input parameters and an energy convergence threshold of 1×10^{-5} eV per cell. Starting from the second generation, 60% structures in the previous generation with the lower enthalpies are selected to produce the structures of next generation by the PSO operators. The 40% structures in the new generation are randomly generated. A structure fingerprinting technique of bond characterization matrix is employed to evaluate each newly generated structure, so that identical structures are strictly forbidden. These procedures significantly enhance the diversity of sampled structures during the evolution, which is crucial in driving the search into the global minimum. For most of cases, the structure search for each chemical composition converges (evidenced by no structure with the lower energy emerging) after 1000 ~ 1200 structures investigated (i.e., in about 20 ~ 30 generations).

To further analyze the structures with higher accuracy, the cut-off energy for the expansion of wave functions into plane waves is set to 620 eV in all calculations, and the Monkhorst–Pack k -mesh with a maximum spacing of 0.02 \AA^{-1} was individually adjusted in reciprocal space with respect to the size of each computational cell. This usually gives total energies well converged very well.

The reliabilities of the projected-augmented-wave (PAW) pseudopotentials for Li and Ag at high pressures, which are used for all the energetic calculations, are crosschecked with the full-potential linearized augmented plane-wave (LAPW) method as implemented in the ELK code. By using two different methods, we calculate total energies of oxygen-richest stoichiometry Li_4Ag in the $I4/m$ structure at varied pressures, and then fit the obtained energy-volume data into the Birch-Murnaghan equation of states. Figure S1 shows the resulted fitted equation of states. We can see the results derived from two methods are almost identical. This clearly indicates the suitability of the PAW pseudopotentials for describing the energetic stabilities of Li–Ag compounds up to 100 GPa.

2. Comparison of PAW pseudopotentials and the LAPW method

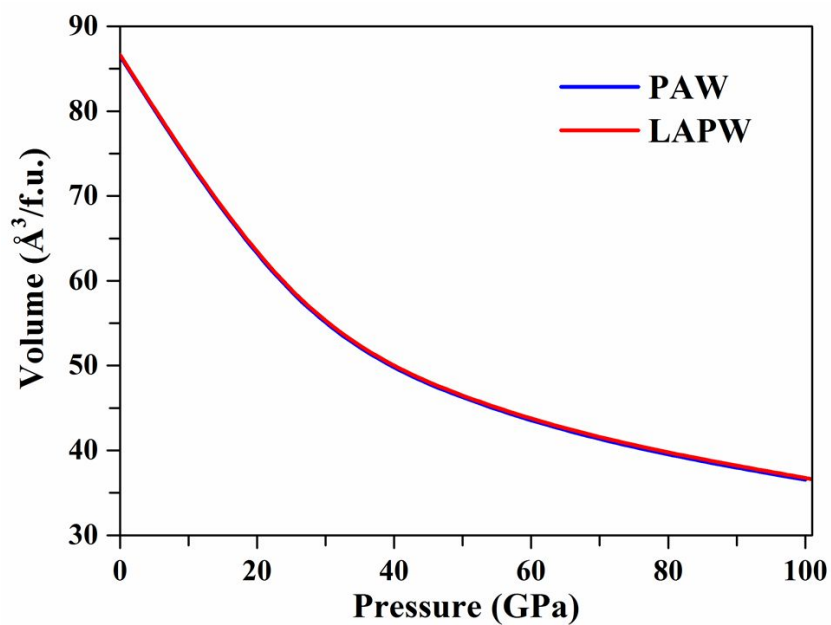


Figure S1. Comparison of the fitted Birch-Murnaghan equation of states for Li_4Ag in the $I4/m$ structure by using the calculated results from the PAW pseudopotentials and the full-potential LAPW method. The perfect match on equation of states supports the validity of PAW pseudopotentials used in Li–Ag compounds up to 100 GPa.

3. Structures of stable Li-rich Li_mAg ($m=1-6$) at high pressures.

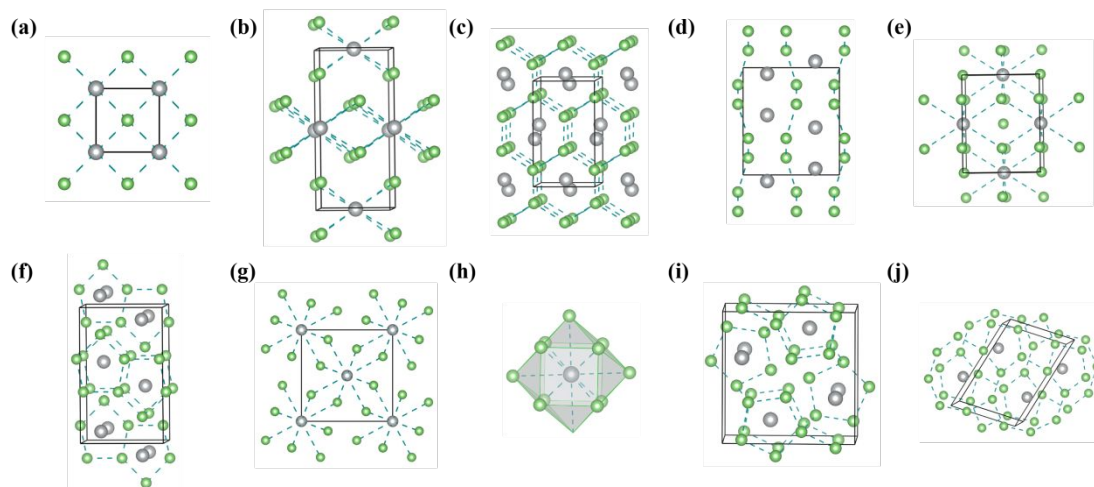


Figure S2. Structures of stable Li-rich Li_mAg ($m=1-6$) at high pressures. (a) The LiAg in the $Pm-3m$ structure; (b) The Li_2Ag in the $Immm$ structure; (c) The Li_2Ag in the $Imcm$ structure; (d) View of corrugated graphene layered pattern in $Imcm$ phase of Li_2Ag ; (e) The Li_3Ag in the $Pmnm$ structure; (f) The Li_3Ag in the $Cmcm$ structure; (g) The Li_4Ag in the $I4/m$ structure; (h) View of a tetra-decahedron in Li_4Ag ; (i) The Li_4Ag in the $Pnnm$ structure; (j) The Li_6Ag in the $P2_1/m$ structure. Small blue and large gray spheres represent Li and Ag atoms, respectively. Solid lines depict the unit cells of the structures.

4. Phonon spectra and dynamic stability

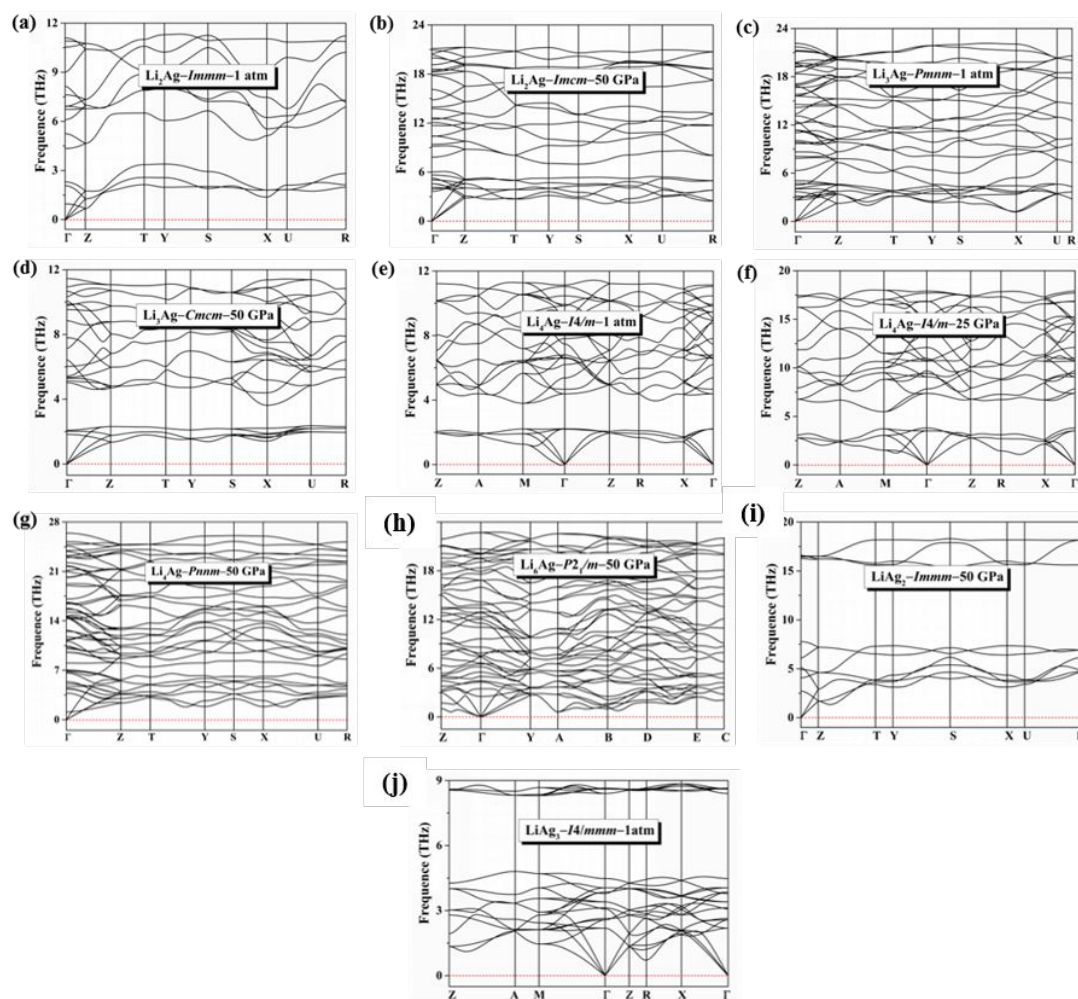


Figure S3. Calculated phonon spectra for various Li-Ag compounds at the respective stable pressure range. There are no imaginary modes for these structures in their stability pressure range, indicating dynamical stability of predicted structures.

5. Two-dimensional ELF plots on (0 0 1) section of Li_4Ag

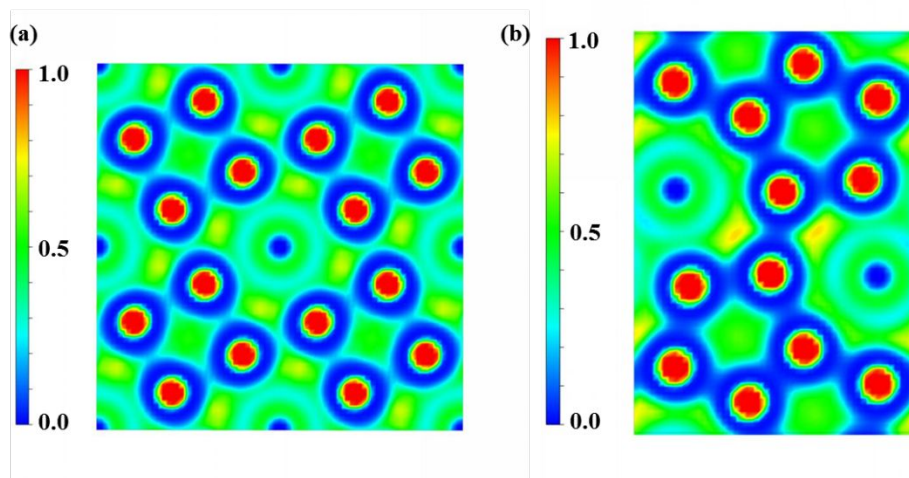


Figure S4. Electron localization functions (ELF) plots showing a (001) cross-section for the $I4/m$ and $Pnnm$ phase of Li_4Ag structures, respectively.

6. Comparison of PDOS of 5p orbital of Ag for Li_4Ag , Li_0In , and Li_0Sn

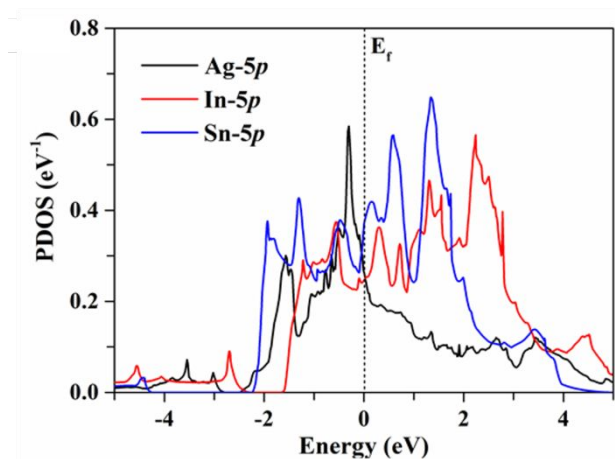


Figure S5. The occupation of the 5p state of Ag in $Pnnm$ phase of Li_4Ag is compared with those of 5p states for In and Sn as modeled by Li_0In and Li_0Sn . The current comparison unambiguously shows that Ag in Li_4Au transforms from transition metal to 5p group element as similar to In and Sn elements.

7. Detailed Structural Information

Table S1. Detailed structural information of the stable Li-Ag compounds at selected pressures.

Phase	Pressure (GPa)	Lattice parameters (Å)		Atomic coordinates (fractional)		
LiAg [<i>Pm-3m</i>]	0	$a = b = c = 3.177$	Li(1b)	0.500	0.500	0.500
		$\alpha = \beta = \gamma = 90.000$	Ag(1a)	0.000	0.000	0.000
LiAg [<i>I4_v/amd</i>]	0	$a = b = 3.956$	Li(4a)	1.000	-0.500	0.250
		$c = 8.382$	Ag(4b)	0.500	0.000	0.250
		$\alpha = \beta = \gamma = 90.000$				
Li₂Ag [<i>Immm</i>]	0	$a = 2.935$	Li(4i)	0.000	0.000	0.839
		$b = 3.973$	Ag(2c)	0.500	0.500	0.000
		$c = 8.548$				
		$\alpha = \beta = \gamma = 90.000$				
Li₂Ag [<i>Imcm</i>]	50	$a = 3.505$	Li(8h)	0.500	0.947	-0.341
		$b = 5.391$	Ag(4e)	0.500	0.250	-0.058
		$c = 5.985$				
		$\alpha = \beta = \gamma = 90.000$				
Li₃Ag [<i>Pnnm</i>]	0	$a = 5.882$	Li1(2a)	0.000	0.000	-0.339
		$b = 4.678$	Li2(4f)	0.248	0.500	-0.183
		$c = 4.919$	Ag(2b)	0.000	0.500	-0.690
		$\alpha = \beta = \gamma = 90.000$				
Li₃Ag [<i>Cmcm</i>]	50	$a = 3.675$	Li1(8f)	0.500	0.120	0.039
		$b = 8.033$	Li2(4c)	0.000	0.803	0.750
		$c = 4.918$	Ag(4c)	0.000	0.088	0.750
		$\alpha = \beta = \gamma = 90.000$				
Li₄Ag [<i>I4/m</i>]	0	$a = b = 6.396$	Li(8h)	0.291	0.894	0.000
		$c = 4.228$	Ag(2b)	0.000	0.000	0.500
		$\alpha = \beta = \gamma = 90.000$				
Li₄Ag [<i>Pnnm</i>]	50	$a = 7.051$	Li1(4g)	0.855	0.971	0.000
		$b = 7.043$	Li2(4g)	0.195	0.313	0.000
		$c = 3.565$	Li3(4g)	0.521	0.646	0.000
		$\alpha = \beta = \gamma = 90.000$	Li4(4g)	0.903	0.593	0.500
			Ag(4g)	0.647	0.849	0.500
Li₅Ag [<i>C2/m</i>]	50	$a = 6.910$	Li1(8j)	0.125	0.293	0.580
		$b = 4.786$	Li2(4g)	0.000	0.213	0.000
		$c = 6.409$	Li3(4i)	0.948	0.000	0.708
		$\alpha = \gamma = 90.000$	Li3(4i)	0.307	0.000	0.135
		$\beta = 81.442$	Ag(4i)	0.312	0.000	0.781
Li₆Ag [<i>P2₁/m</i>]	50		Li1(2e)	0.143	0.750	0.434
		$a = 6.910$	Li2(2e)	0.610	0.750	0.920
		$b = 4.785$	Li3(2e)	0.672	0.750	0.471
		$c = 6.409$	Li4(2e)	0.908	0.750	0.802
		$\alpha = \gamma = 90.000$	Li5(2e)	0.442	0.750	0.327
		$\beta = 81.442$	Li6(2e)	-0.063	0.750	0.198
			Ag(2e)	0.280	0.750	-0.132
LiAg₂ [<i>Immm</i>]	25	$a = 2.879$	Li(2b)	0.500	0.000	0.000
		$b = 2.889$	Ag(4j)	0.000	0.500	0.849
		$c = 9.345$				
		$\alpha = \beta = \gamma = 90.000$				

LiAg₃ [<i>I4/mmm</i>]	0	a = b = 4.128	Li(2b)	0.000	0.000	0.500
		c = 8.001	Ag1(4d)	0.000	0.500	0.250
		$\alpha = \beta = \gamma = 90.000$	Ag2(2a)	0.500	0.500	0.500